Quantitative SERS sensor for mycotoxins with extraction and identification function

Yang Zhang [a], Chuping Zhao [a], Pierre Picchetti [b], Kaiyi Zheng [a], Xinai Zhang [a], Yanling Wu [a], Ye Shen [a], Luisa De Cola [b,c,d], Jiyong Shi [a], Zhiming Guo [a,*], Xiaobo Zou [a,*]

[a] International Joint Research Laboratory of Intelligent Agriculture and Agriproducts Processing, China Light Industry Key Laboratory of Food Intelligent Detection & Processing, School of Food and Biological Engineering, Jiangsu University, Zhenjiang, Jiangsu 212013, China
[b] Institute of Nanotechnology (INT), Karlsruhe Institute of Technology (KIT), Kaiserstrasse 12, 76131 Karlsruhe, Germany
[c] Department DISFARM, University of Milano, via Camillo Golgi 19, 20133 Milano, Italy
[d] Department of Molecular Biochemistry and Pharmacology, Istituto di Ricerche Farmacologiche Mario Negri IRRCCS, 20156 Milano, Italy

Keywords:
Food safety
SERS
Sensor
Mycotoxins

A B S T R A C T

The development of new sensors for on-site food toxin monitoring that combine extraction, analytes distinction and detection is important in resource-limited environments. Surface-enhanced Raman scattering (SERS)-based signal readout features fast response and high sensitivity, making it a powerful method for detecting mycotoxins. In this work, a SERS-based assay for the detection of multiple mycotoxins is presented that combines extraction and subsequent detection, achieving an analytically relevant detection limit (~ 1 ng/mL), which is also tested in corn samples. This sensor consists of a magnetic-core and mycotoxin-absorbing polydopamine-shell, with SERS-active Au nanoparticles on the outer surface. The assay can concentrate multiple mycotoxins, which are identified through multiclass partite least squares analysis based on their SERS spectra. We developed a strategy for the analysis of multiple mycotoxins with minimal sample pretreatment, enabling in situ analytical extraction and subsequent detection, displaying the potential to rapidly identify lethal mycotoxin contamination on site.

1. Introduction

Human food poisoning caused by mycotoxins from fungal pathogens is a global concern that has serious economic and environmental negative impacts on the agricultural sector and food safety (Avery et al., 2019; D. Huang et al., 2021). The number of deaths caused by mycotoxins from contaminated foods such as dried fruits, grains, nuts, and spices is estimated at 1.6 million per year, with more than one billion people suffering from non-lethal poisoning (Almeida et al., 2019; Casadevall, 2018; Molloy et al., 2017). Indeed, the Food Agricultural Organization (FAO) reports high levels of mycotoxin contamination in food, originally estimated at around 25% of global food crops (D. Huang et al., 2021), with around 60–80% having mycotoxins above detectable levels (Eskola et al., 2020), of which corn is one of the most commonly contaminated foods (Munkvold et al., 2019). To avoid major economic damage or serious health risks, the detection of mycotoxins should ideally be carried out quickly and with high sensitivity on-site (Kasoju, Shahdeo, et al., 2020; Kasoju, Shrikrishna, et al., 2020).

Among mycotoxins, aflatoxin B_1 (AFB_1), ochratoxin A (OTA), and deoxynivalenol (DON) are commonly found in spoiled foods (Bräse et al., 2009; H. J. Lee et al., 2015) and their maximum acceptable levels (action levels) in foods are regulated by the World Health Organization (WHO), European Commission, US and China, for example that of AFB_1, OTA and DON by EC regulations are 2, 200 (in baby foods), 2(in wine) μg/Kg, respectively, the more details can be seen in Table S4. Up to date, the gold standard method for the detection of mycotoxins relies on high-performance liquid chromatography and mass spectroscopy (HPLC-MS) (Mahoney & Molyneux, 2010), whereas also other detection methods exist, e.g., immunoassays (enzyme-linked immunosorbent assay, fluorescent immunoassay) (Shengyang Zhou et al., 2020), or antibody (X. Huang et al., 2016) and aptamer-based nanosensors (Xiong et al., 2022). Although some of these analytical techniques meet the standards required for the accurate detection of various mycotoxins, they are not well suited for rapid on-site detection in low resource settings. For example, the analysis of potentially spoiled food requires laborious pre-processing steps if HPLC-based detection methodologies are utilized. In addition, HPLC is impractical for on-site detection, especially in remote areas. Therefore, developing a novel strategy to overcome these

* Corresponding author at: School of Food and Biological Engineering, JiangSu University, 301 Xuefu Rd, Zhenjiang 212013, Jiangsu, China.
E-mail address: zou_xiaobo@ujs.edu.cn (X. Zou).

shortcomings is of great interest.

Considerable progress has been made in the area of detection methods through the integration of nanomaterials (Aragay et al., 2012; L. Yang et al., 2021). The inherent properties of nanomaterials, such as their small size, large surface-to-volume ratio and superior physicochemical properties, together with their distinct target binding capabilities, have significantly improved the specificity and sensitivity of detection methods. For example, magnetic nanoparticles have been used to isolate and concentrate aflatoxins for subsequent analysis by high-performance liquid chromatography-mass spectrometry (HPLC-MS), simplifying sample preparation from complex food matrices (McCullum et al., 2014). In addition, antibodies and aptamers in combination with nanoparticles have been widely used for the detection and identification of mycotoxins in food samples. (J. Li et al., 2020; X. Liu et al., 2019; Yin et al., 2022). Nevertheless, antibody-based detection methods for mycotoxins, although effective, are problematic in terms of cost and stability, especially for on-site detection applications (D. Huang et al., 2021; Xiong et al., 2022). So, it is significant to develop a detection method with lower cost, more stable and easier preparation steps. Nanosensors using SERS as a signal readout are interesting because they can provide specific "fingerprint" spectra of analytes that can be analyzed for qualitative and quantitative detection in complex environments, and achieve excellent detection limits. Indeed, SERS fingerprinting-based detection has been widely used in the detection of chemicals (Kasera et al., 2012; Phan-Quang et al., 2017), biomarkers (Panikkanvalappil et al., 2019; Y. Zhang et al., 2018), and more complex targets such as bacteria (S. Zhou et al., 2022), archaea (Y. Wang et al., 2021), and cells (Lenzi et al., 2022) and in combination with chemometric analyses, e.g. machine learning algorithms, high-throughput measurements of complex analyte mixtures can be analyzed with high accuracy (Ding et al., 2023; dos Santos et al., 2023; Ho et al., 2019). Among these statistical techniques, principal component analysis (PCA), linear discriminant analysis (LDA), and partial least squares regression (PLS) are commonly used for dimensionally reduction, which extract key indicators from complex data for classification and regression analysis (Kutsanedzie et al., 2020; F. Wang et al., 2023). Multiclass partial least squares-discriminant analysis (MPLSDA) is a popular classification method that is based on the PLS approach, where the final predication results depend on all the submodels. Additionally, DA analysis is to create a discriminant model by utilizing the samples of know categories, to identify the unknown samples, to minimize wrong judgment (Feng et al., 2015; Pomerantsev & Rodionova, 2018).

With respect to mycotoxin detection, the most sensitive detection capabilities have been realized through the application of SERS tagging techniques using plasmonic nanoparticles functionalized with antibodies or aptamers (Y. Yang et al., 2022; W. Zhang et al., 2020; Zhao et al., 2015). These methods take advantage of the high affinity between the target mycotoxin and the SERS-based nanosensor, resulting in high sensitivity and specificity for individual mycotoxin analysis. Despite these advances, the ability of detecting multiple mycotoxins with one nanosensor is a major challenge. For the detection of multiple mycotoxins, maintaining a balance between affinity and multiplex detection in one sensor is important(Wu et al., 2021). Developing an effective receptor for the detection of multiple mycotoxins, which have a high affinity and is robust in harsh environment, presents a challenge. In this sense, polydopamine (PDA), known for its high affinity to mycotoxin molecules and its superior stability in complex solutions, proves to be a viable alternative to antibody/aptamer-based mycotoxin recognition units (Dai et al., 2022; Wan et al., 2017; L. Wang et al., 2019). Given the complexity of food samples and the need to detect mycotoxins, the development of robust, easy-to-use SERS-active nanosensors capable of extraction, identification and detection is important (Andreasen et al., 2018; Z. Liu et al., 2016; McCullum et al., 2014). However, to the best of our knowledge, there are no reports of a nanoparticle-based SERS detection method that allows the extraction of mycotoxins in food samples and their subsequent differential detection with the required sensitivity.

In this work, we present a SERS-based nanosensor assay which provides rapid extraction, discrimination, and detection of mycotoxins (aflatoxin B_1, ochratoxin A, and deoxynivalenol) with a limit of detection (LOD) of ~1 ng/mL (Scheme 1). We accomplished this through a nanoparticle preparation strategy in which the mycotoxins present in a sample are anchored in a polydopamine shell that surrounds magnetic core nanoparticles. The subsequent deposition of Au nanoparticles on the polydopamine layer creates the necessary "hot spots" for SERS-based detection. This method enables the identification of adsorbed mycotoxins based on their unique spectral fingerprints. Importantly, no special pretreatment of the food sample is required for mycotoxin detection other than a simple filtration step. To analyze the complex and similar Raman spectra of mycotoxins, a machine learning categorization model based on multiclass-partial least square discrimination analysis (MPLSDA) was employed and the method enable the identification of three mycotoxins in corn samples with accuracies ≥93%. Overall, our results show that this multifunctional SERS platform is effective against mycotoxins and can extract, discriminate, and detect multiple mycotoxins, reaching the detection limits required by food authorities. This is significant for multiple and rapid detection. Since the nanosensor also works in complex food samples, we can foresee it being applicable in drug testing, food safety, and medical diagnostics.

2. Experiments

2.1. Materials and instruments

Ethylene glycol, ethanol, Iron(III) chloride hexahydrate ($FeCl_3{\cdot}6H_2O$), tris hydrochloride, sodium citrate dihydrate, gold (III) chloride hydrate, anhydrous sodium acetate, hydroxylamine hydrochloride, sodium hydroxide (NaOH), dopamine hydrochloride, methanol, and hydrochloride were purchased from Sinopharm. All reagents were of analytical reagent grade (≥99.0%). The mycotoxins including aflatoxin B_1 (AFB_1), deoxynivalenol (DON), and ochratoxins A (OTA) were provided by Sigma Aldrich and used as received. Silicon wafer (single slide polished) was obtained by Sigma Aldrich. Water (resistivity of 18.2 MΩ•cm) was purified by a Milli-Q system.

The morphologies of nanoparticles were characterized using scanning electron microscopy (SEM, Hitachi Regulus 8100). The samples were prepared by drop-casting aqueous solutions of nanoparticles on an SEM holder (0.5 mg/mL), and the samples were dried at ambient pressure. The normal transmission electron microscopy (TEM) images were obtained by a JEM-2100 (JEOL, Japan), and samples were prepared by immersing a graphite-coated copper grid into the nanoparticle solution (1 mg/mL). The high-angle annular dark-field (HADDF) images and energy-dispersive X-ray (EDX) maps were obtained by a TF20 (FEI company, USA). Dynamic light scattering (DLS) and Zeta potential measurements were carried out with a Zetasizer Nanoseries (Brookhaven, Nano ZS90, USA). Thermogravimetric analyses (TGA) were performed on a Perkin-Elmer Thermogravimetric Analyzer (Q5000). Samples were heated from room temperature to 800 °C (rate, 20 °C/min, air as furnace gas). An XploRA Nano Raman spectrometer (HORIBA France SAS) was used to record the Raman data. The SERS spectra were obtained using a laser of 638 nm with 10% power, 10 X objective, and a 1200 g/mm grating, where the exposure time was 10 s with 5 accumulations for each measurement. Fourier transform infrared spectra (FTIR) were measured on a Nicolet iS20 Fourier transform infrared spectrometer (Thermo Fisher Scientific) equipped with attenuated total reflectance (ATR), over the range of 500–4000 cm^{-1}. High-performance liquid chromatography (HPLC) analyses were performed on an LC-20 CE system (Shimadzu, Japan) equipped with two pumps, fluorescent detector, and UV–vis detector. All the measurements were repeated by three times and the average value and deviation were calculated as the final data.

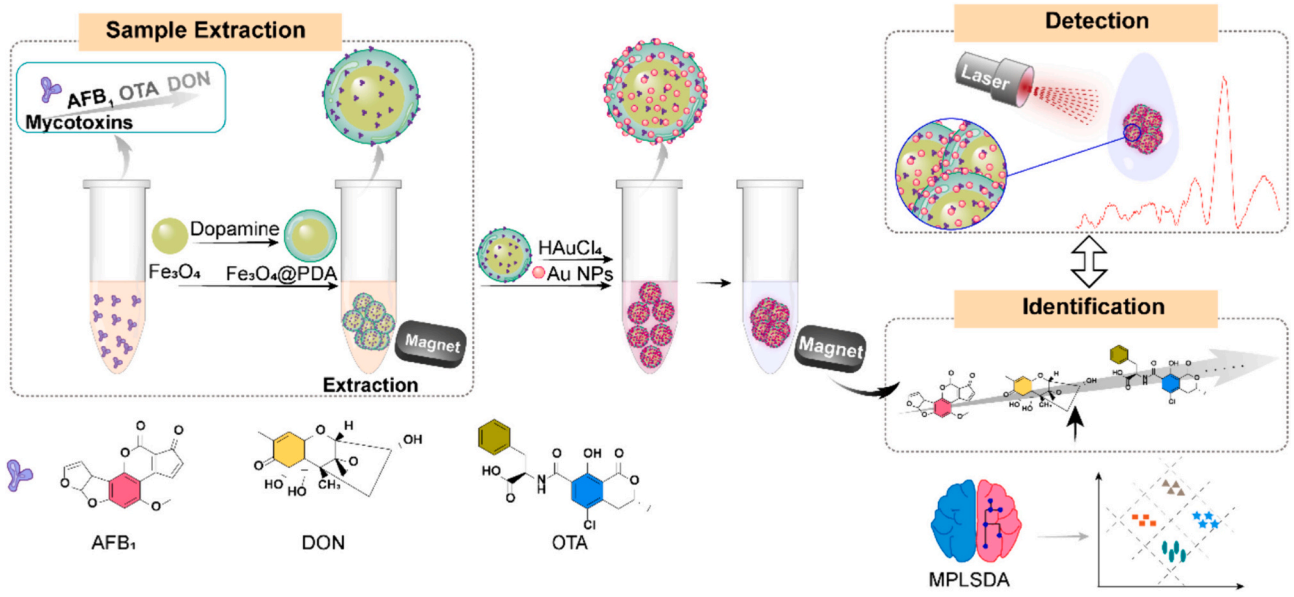

Scheme 1. A schematic representation of the operating principle of the SERS-based nanosensor for mycotoxins detection.

2.2. Preparation of magnetic nanoparticles modified by poly-dopamine (Fe_3O_4@PDA)

Fe_3O_4 nanoparticles were prepared according to the literature with slight modifications (J. Liu et al., 2009; Zheng et al., 2015). Briefly, 2.17 g of $FeCl_3{\cdot}6H_2O$ (8 mmol), 0.4 g of sodium citrate dihydrate (1.4 mmol) and 2.4 g of sodium acetate (29 mmol) were dissolved into 40 mL of ethylene glycol with stirring at 50 °C for 30 min until a homogenous dispersion formed. Then the mixture was transferred into a teflon-lined stainless-steel autoclave (100 mL capacity) sealed and heated at 200 °C for 10 h. Subsequently, the autoclave was allowed to cool to room temperature and the precipitate was washed with ethanol (3 × 90 mL) and with water (3 × 90 mL). Finally, the black precipitated (Fe_3O_4 NPs) was lyophilized (yield ~100 mg).

The poly-dopamine-coated magnetic nanoparticles (Fe_3O_4@PDA) were synthesized by adapting a previously reported oxidative self-polymerization procedure (Zheng et al., 2015). Briefly, 20 mL of Tris-HCl buffer (10 mM, pH 8.5) was used to disperse 40 mg of the Fe_3O_4 nanoparticles via short sonication (30 s, 50 w, 40 kHz). Then 40 mg of dopamine hydrochloride was added to the particle dispersion and the dispersion was sonicated. The resulting dispersion was split into 4 equal parts. Each dispersion was gently stirred in an orbital shaker and reacted for 6 h at room temperature. The resultant products were washed 4× with water (30 mL) and collected by a magnet. The obtained Fe_3O_4@PDA (yield ~70 mg) nanocomposites were lyophilized for further use.

2.3. Preparation of mycotoxins samples

Different concentrations of AFB_1, DON, and OTA were prepared by diluted standard solutions with methanol and water (see Supporting information). The mycotoxin-spiked corn samples were prepared as follows: 5 g of dried corn was grounded to a fine powder. Then the powder was suspended in a methanol-water (*v*/v, 70/30) mixture, and sonicated for 10 min. The solids were removed by filtration (8000 rpm, 20 min), and AFB_1, DON, and OTA standard samples with various concentrations were added to the supernatant, respectively. The mycotoxin-spiked corn samples were used as application-appropriate samples to mimic the real environment for further detection.

2.4. Extraction of mycotoxins

The mycotoxins stock solutions (AFB_1 1 mg/mL in Acetonitrile, OTA 0.1 mg/mL in Methanol, DON 0.01 mg/mL in Acetonitrile) were used. The work solutions of different mycotoxins with different concentrations were freshly obtained by appropriated dilution with water/methanol (50/50, *v*/v). To a plastic centrifuge tube containing 7 mg of solid Fe_3O_4@PDA, 5 mL of a mycotoxin work solution was added. The mixture was sonicated for 1 min to disperse the nanoparticles, followed by shaking on a rotatory shake for 25 mins. The nanoparticles were settled down by being placed on a magnet and the supernatant was transferred to another clean tube. For the MPLSDA analysis, each mycotoxin had 30 samples, which were divided into three groups averagely. The three groups were corresponding to three concentrations 3, 5, 10 ng/mL. After extraction and separation with a magnet, the mycotoxin in the supernatant was quantified by HPLC, and the extraction efficiency was calculated. (Mahoney & Molyneux, 2010). In the HPLC analysis of mycotoxins, a C18 column (ShimNex CS C18, 5 μm particle size, 4.6 × 250 mm) was used for detecting the residue of mycotoxins in the supernatant. The mobile phase was composed of methanol and water (*v*/v, 60/40) at a constant flow rate of 0.6 mL/min. The sample injection volume was 15 μL.

The extraction efficiency was calculated by the following equations:

$$E = \frac{(C_0\text{-}C)}{C_0} \times 100\%$$

where C_0 (μg/L) and C (μg/L) are the concentration of mycotoxin in the solution before and after the addition of magnetic nanoparticles (Fe_3O_4@PDA).

2.5. In situ preparation of au nanoparticles and SERS measurements

After the magnetic nanoparticles absorbed mycotoxins (Fe_3O_4@PDA@MT), they were collected by a magnet and dispersed in 5 mL of water. Subsequently, 500 μL of $HAuCl_4$ (5 mM), and 500 μL of hydroxyl amine hydrochloride (50 mM) were added to the particle dispersion consecutively, and the reaction mixture was mixed by sonication and incubated for 10 min at room temperature. The Au nanoparticles, as a Raman-enhancing substrate, were formed on the surface of Fe_3O_4@PDA@MT in situ, to form the final magnetic - plasmonic gold - nanocomplex (which is abbreviated as MPNc). The MPNc were separated by a

magnet and transferred to a silicon slide (1 cm × 1 cm) for subsequent SERS measurements. For each sample, 6 random spots were chosen for obtaining the Raman spectra, and the SERS result was got by average of these 6 spectra. Based on the SERS results, the data from solution samples diluted from mycotoxins stock solutions was used to calculate the linearity, while the data from mycotoxin spiked corn samples were used to obtain the recovery rate.

2.6. Statistical analysis

The smooth, baseline correction of SERS spectra were performed in LabSpec 6 (Horiba Scientifics, France) software based on polynomial fitting. The analysis of multiclass partial least square discrimination analysis (MPLSDA) was obtained by using SIMCA 14.0 software. Three batches of spectra were set as X, and the corresponding category labels were set Y. The Y consisted of three column vectors, where each one can be seen as one class. In each vector, if the samples belonged to this class, the samples were assigned as one, whereas as zeros. After calibration, the calibrated model was applied to prediction. In prediction, the predicted label of one sample could be shown as a row vector. In this row vector, the location of the element above 0.5 could be applied to identifying the corresponding class. The more details were put in supporting information.

3. Results and discussion

3.1. Characterization of Fe_3O_4@PDA

Iron oxide nanoparticles (Fe_3O_4) were chosen as the magnetic core for our nanosensor as they can magnetically separate from the bulk solution. This will facilitate the recovery of the nanosensor from food samples, which are then analyzed using SERS to detect mycotoxins (Scheme 1). The citrated-capped Fe_3O_4 NP were prepared by modifying a previously reported procedure.(J. Liu et al., 2009) TEM images showed that the Fe_3O_4 nanoparticles have a spherical shape (Fig. 1a, Fig. S2) with an average diameter of 210.9 ± 34.6 nm (Fig. 1b). Dynamic light scattering analysis revealed that the hydrodynamic diameter of Fe_3O_4 was 231.2 ± 12.9 nm with a polydispersity index (PDI) of 0.22 ± 0.02 (Fig. 1c, red line). Zeta potential measurements of the particles revealed a negative surface (25.2 ± 0.5 mV) charge due to the citrate on the surface of the particles, which is also responsible for the good stability of the particle dispersion (Fig. S3).

Next, a suitable method for forming a PDA shell around the Fe_3O_4 nanoparticles by oxidative polymerization of dopamine in basic media (Tris buffer, pH = 8.5) was aimed for. The deposition and polymerization of dopamine around the Fe_3O_4 core particles is driven by the electrostatic interaction between the negatively charged citrate groups of the nanoparticles and the positively charged -NH_3^+ groups of dopamine, and this is also enhanced by the hydrogen bonding between the citrate groups of the magnetic nanoparticles and the catechol group of dopamine (Choi et al., 2019; Sun et al., 2018). We were pleased to see that, as shown in Fig. 2a, a PDA shell was successfully formed around the core of Fe_3O_4 nanoparticles (see Supporting Information), resulting in a well-defined spherical core-shell structure (Fig. 2a) of PDA-functionalized particles (Fe_3O_4@PDA) with a PDA shell thickness of 31.9 ± 3.2 nm. The hydrodynamic diameters of the particles increased compared to the Fe_3O_4-nanoparticles to 640.5 ± 15.3 nm due to particles aggregation (Fig. 1c, blue line). Additionally, the zeta potential increased to 8.3 ± 0.7 mV owing to the catechol groups from the PDA shell (Fig. 1d).

3.2. Adsorption of mycotoxin

TGA was used to quantitatively estimate the amount of organic content in Fe_3O_4@PDA and Fe_3O_4. Fig. 2b shows that a 10.6 wt% weight loss was observed for the Fe_3O_4 nanoparticles, which can be attributed to the presence of the citrate groups on their surface. After PDA functionalization a 36.9 wt% loss in weight was observed, mainly due to the presence of the PDA shell. The presence of the PDA in Fe_3O_4@PDA nanoparticles was further confirmed via attenuated total reflectance

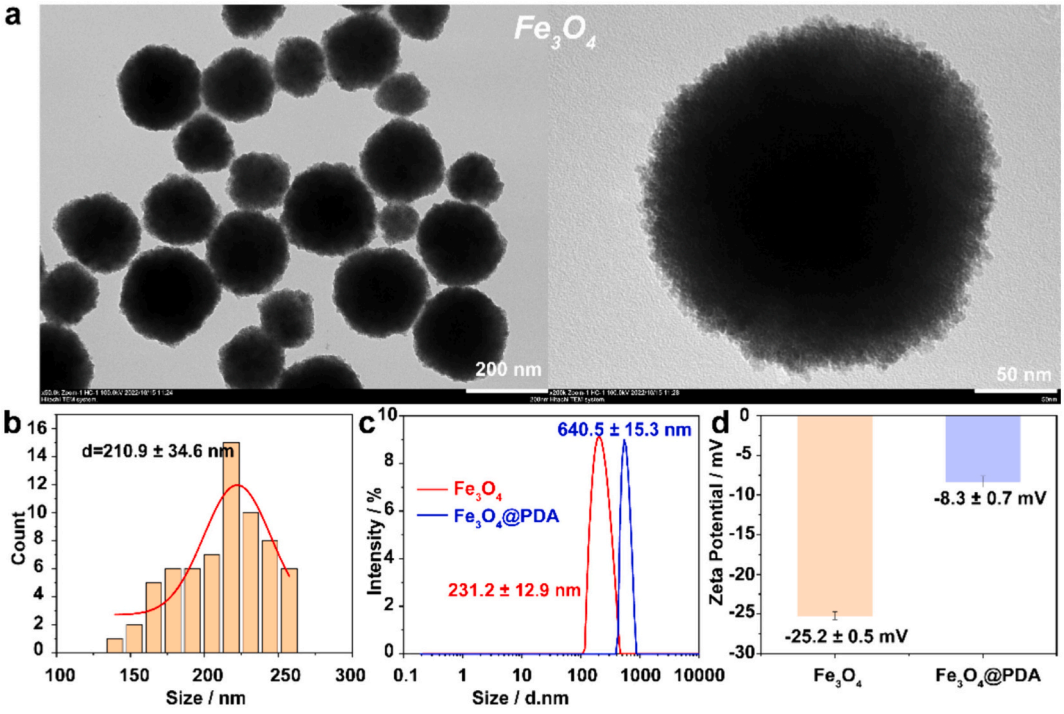

Fig. 1. (a) The TEM images of Fe_3O_4 nanoparticles. (b) The size distribution of Fe_3O_4 nanoparticles, with an average size of 210.9 ± 34.6 nm. (c, d) The DLS size and zeta potential of Fe_3O_4 nanoparticles (red line) and the nanoparticles covered by the polydopamine shell (Fe_3O_4@PDA, blue line). (For interpretation of the references to color in this figure legend, the reader is referred to the web version of this article.)

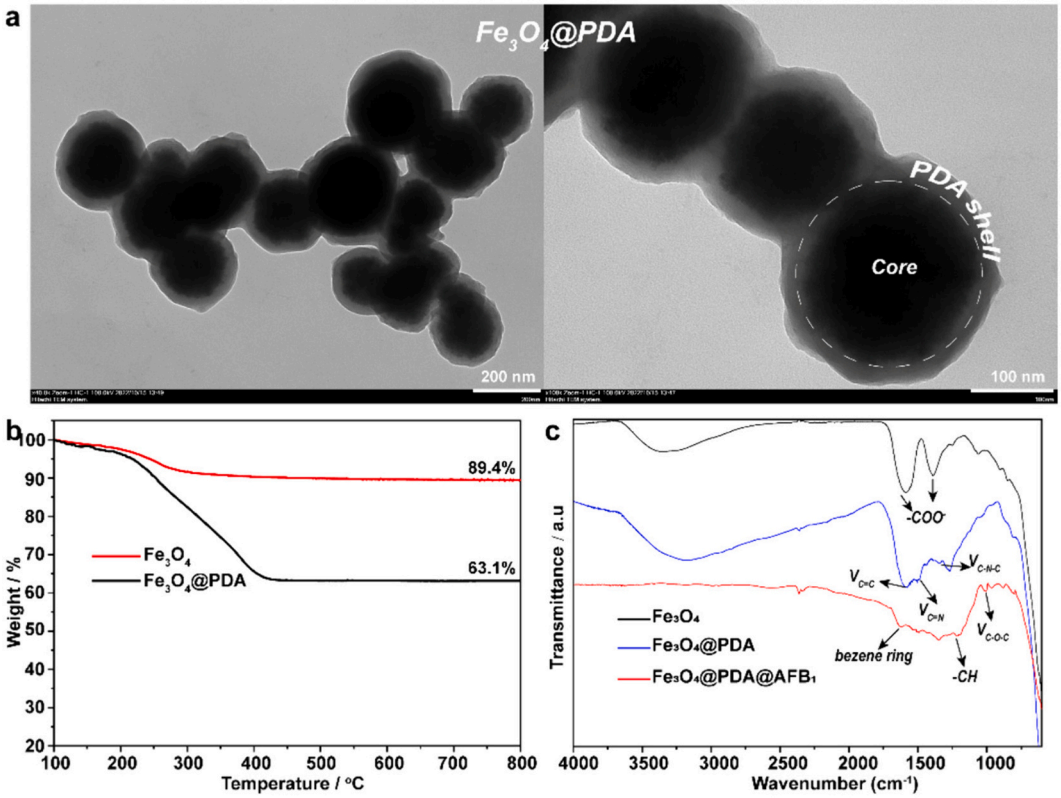

Fig. 2. (a) The TEM images of Fe_3O_4@PDA nanoparticles. (b) TGA curves of Fe_3O_4, and Fe_3O_4@PDA. (c) The ATR-FTIR spectra Fe_3O_4 nanoparticles, Fe_3O_4@PDA nanoparticles, and Fe_3O_4@PDA@AFB_1 nanoparticles.

Fourier transform infrared spectroscopy (ATR-FTIR) shown in Fig. 2c. While the citrate-capped Fe_3O_4 showed the characteristic -COO- transmission bands (1390 and 1587 cm^{-1}) in the FTIR-ATR spectrum, the Fe_3O_4@PDA nanoparticles additionally possessed the transmission bands at 1575 cm^{-1} (C=C), 1506 cm^{-1} (C=N) and 1344 cm^{-1} (C-N-C), which are characteristic bonds of PDA (Yu et al., 2018).

After preparing the Fe_3O_4@PDA, we investigated the interaction of the nanoparticles with mycotoxins. PDA coating consists of planar oligomers that is stacked together based on π-π interactions, producing graphite-like layered aggregates (Ye et al., 2011). The PDA exhibit highly delocalized π-π conjugated system, active groups, hydrophilicity, and large specific surface area. PDA materials have been used widely for developing numerous sorption-based extraction methods and applied to enrich mycotoxins in food samples for further analysis (Che et al., 2017). Chemical adsorption is common adsorption method based on interactive chemical reactions, others like boronate affinity material and cis-diols containing molecules (Q. Li et al., 2023). PDA comprises dopamine units, indoledione, and dihydroxyindole, which contains abundant aromatic rings, phenolic hydroxyl, and amino groups, which can provide hydrogen bonding, electrostatic and π-π stacking interactions with mycotoxin molecules, as an effective adsorbent (Dai et al., 2022; Liebscher et al., 2013; McCullum et al., 2014). To this end we mixed a dispersion of Fe_3O_4@PDA (1.4 mg/mL) with AFB_1(10 ng/mL) for 25 min and collected the particles subsequently with the use of a magnet. The adsorption of the aflatoxin onto Fe_3O_4@PDA was investigated via ATR-FTIR analysis. The new transmission bands occurring at 1015 cm^{-1} (V_{C-O-C}, symmetric, phenyl), 1210 cm^{-1} (-CH, deformation modes), and 1623 cm^{-1} (stretching of benzene ring) can be assigned to AFB_1 (Fig. 2c) (K. M. Lee et al., 2015).

The extraction efficiencies were investigated via HPLC measurements of the supernatants. We investigated the influence of the amount of Fe_3O_4@PDA used to adsorb the mycotoxin. In a set of tests, 1, 3, 5, 7, and 10 mg of Fe_3O_4@PDA were added to different 5 mL portions of a solution containing 10 ng/mL AFB_1 (This value was chosen based on the maximum level of FDA (20 ng/g) and lower than it, to investigate whether this sensor was much sensitive and fit the regulations (see Supporting information for further details and Fig. S4a, 4c, 4e). We observed that the extraction efficiency for AFB_1 increased from 40.1 ± 3.0% to 83.2 ± 3.9% with increasing the amount of Fe_3O_4@PDA, and the efficiency reached a plateau when >5 mg of Fe_3O_4@PDA was used. The similar results were also obtained in the extraction of OTA, and DON, the maximum efficiency are 86.3 ± 1.1% and 81.5 ± 1.5% for OTA and DON, respectively. To keep the operational consistency, 7 mg of Fe_3O_4@PDA was used to extract mycotoxins in 5 mL solutions. The influence of extraction times (5, 10, 15, 20, and 25 min) was also evaluated. The maximum extraction efficiency of AFB_1 got 81.9 ± 1.5%, after 25 min (Fig. S4b), while it also got the maximum for OTA (86.9 ± 1.6%) and DON (81.5 ± 2.1%) during this time (Fig. S4d, 4f). Fig. S5 shows the original results of the HPLC test of each mycotoxin under the optimum conditions, the peak area drastically decreased after the adsorption of Fe_3O_4@PDA (Table S2). In these three mycotoxins, we found the DON has lower dosage of nanoparticles and shorter adsorption time to get the maximum, this might be because of lower molecule weight of DON (296.3) compared with AFB_1 and OTA. The optimized conditions for the extraction of mycotoxins are obtained by using 1.4 mg/mL of Fe_3O_4@PDA (this was equal to 7 mg of nanoparticles, if the volume is 5 mL) and 25 min of incubation time, these parameters were used for the following SERS-based sensing. Under this condition, we also tested the selectivity of Fe_3O_4@PDA toward the other three mycotoxins that we have, Patulin (PAT), Citrinin (CIT), and Alternariol (AOH) by HPLC analysis. The spectrum kept the same before and after the adsorption of Fe_3O_4@PDA (Fig. S6). The results show the Fe_3O_4@PDA has negligible adsorption to these three mycotoxins (Table S3).

3.3. Formation of SERS substrate

Once the optimal parameters for mycotoxin adsorption were determined, the next step was to functionalize the surface of Fe_3O_4@PDA (after mycotoxin extraction) with SERS-active Au nanoparticles to obtain the final SERS-active nanoparticles. We used hydroxylamine hydrochloride as a reducing agent for achieving a mild, efficient formation of Au nanoparticles (Kumar et al., 2014). At first, the reduction process of Au(III) ions involves the oxidation of catechol to quinone of the PDA shell, forming Au(0), which is deposited on the surface of the PDA shell and forms the first Au nuclei. In a subsequent step, additional hydroxylamine was added to reduce the remaining $AuCl_4$ ions, which promotes the growth of Au nanoparticles and prevents further reaction with catechol. The resulting nano complex (Fe_3O_4@PDA@Au with mycotoxin, namely MPNc) has exhibited characteristic red-color, and the UV–Vis spectra showed an absorption maximum at 648 nm (Fig. 3b, inset for details). Scanning electron microscopy (SEM) images confirmed the dense distribution of Au nanoparticles on the PDA-coated Fe_3O_4 surface (Fig. 3c), while transmission electron microscopy (TEM) images showed Au nanoparticles on the outermost layer of Fe_3O_4@PDA particles (Fig. S7a). Energy dispersive X-ray (EDX) analysis showed the existence of C, Fe, and Au elements, which are corresponding to the polydopamine and mycotoxin, Fe_3O_4 and Au. High-angle annular dark-field (HAADF) imaging and corresponding elemental mapping showed the uniform distribution of Au nanoparticles on the surface (Fig. S7b-f).

SERS measurements revealed a significant enhancement in the Raman signal of Fe_3O_4@PDA@Au compared to the Fe_3O_4 nanoparticles with only a PDA coating, suggesting the enhanced performance of the assay as a SERS sensor (Fig. S8). Finite-Difference Time-Domain (FDTD) simulations indicated strong local electromagnetic fields around the Au nanoparticles, attributed to their discrete and proximal arrangement on the surface (Fig. S7h, 7i) The SERS spectra of PDA resembled those found in prior studies, with two distinctive bands at 1395 cm^{-1} and 1572 cm^{-1} corresponding to the deformation and stretching of aromatic rings, respectively(Cortés et al., 2019; Ma et al., 2015).

3.4. Identification of mycotoxins by MPLSDA analysis

First, we further tested the selectivity of Fe_3O_4@PDA to other pesticides under the optimal conditions for mycotoxins. These pesticides are very common in agricultural products, including Isocarbophos, Imidacloprid, Iprodione, Chlorpyrifos and Thiabendazole. Each chemical had two testing concentrations, which were varied dependent on the official standards; from the HPLC analysis, Fe_3O_4@PDA had much lower extraction efficiency toward these pesticides (< 10%) (Table S5). The extraction efficiency toward Thiabendazole (4 ng/mL) was 9.1 ± 1.5%, and this for Chlorpyrifos (1 ng/mL) was 0.3 ± 0.1%, while the extraction efficiency to others were between these two values. These results showed the Fe_3O_4@PDA had good selectivity toward mycotoxins, and we concluded that the Fe_3O_4@PDA could adsorb mycotoxins efficiently.

Then, we collected the SERS spectra of MPNc (Fe_3O_4@PDA@Au with mycotoxin), every mycotoxin had 30 replications (30 samples). The SERS spectrum include the information from polydopamine and mycotoxin, eg, for AFB_1 it had the molecule information of polydopamine and AFB_1. But, as the high degree of similarity among the SERS spectra of mycotoxins and each MPNc, it was difficult to distinguish each other by visual inspection (Fig. S9). So, a chemometric method was processed to identify different mycotoxins automatically and accurately by using MPLSDA (the more details were described in the supporting information). 90 Raman spectra of mycotoxins respectively, obtained by this nano sensor, including 30 AFB_1, 30 DON and 30 OTA samples were divided as calibration and prediction sets randomly. In each random division, 15 AFB_1, 15 DON and 15 OTA samples were used to calibrate the model, while the residual samples were to predict. Fig. S1 shows the 2-fold cross validation of mycotoxin, the prediction results of each mycotoxin are all nearly 1 (Table S1). This shows the high prediction accuracy. Moreover, in order to further analyze the results of cross validation, the calibration and prediction set were randomly generated. After generation, the prediction accuracy can be predicted by cross validation. After repeated running 100 times, the average prediction accuracy of three batches of samples were all above 93%, which are shown in Fig. 4. This indicated that the MPLSDA analysis was able to

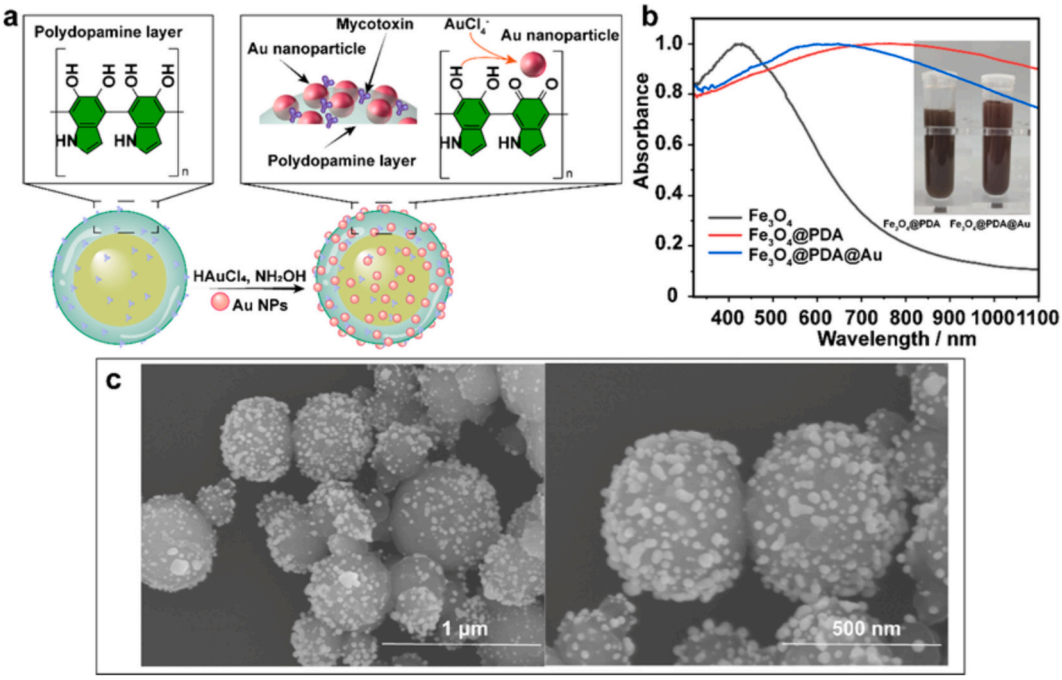

Fig. 3. (a) Schematic representation of the polydopamine layer and the oxidative process of polydopamine on Fe_3O_4 nanoparticles for the synthesis of Au NPs. (b) The UV–vis spectra of Fe_3O_4, Fe_3O_4@PDA, and MPNc nanoparticles. Inset: the image of Fe_3O_4@PDA nanoparticles with the absorption of mycotoxin, and the images of MPNc solution (1.4 mg/mL). (c) The SEM images of MPNc nanoparticles.

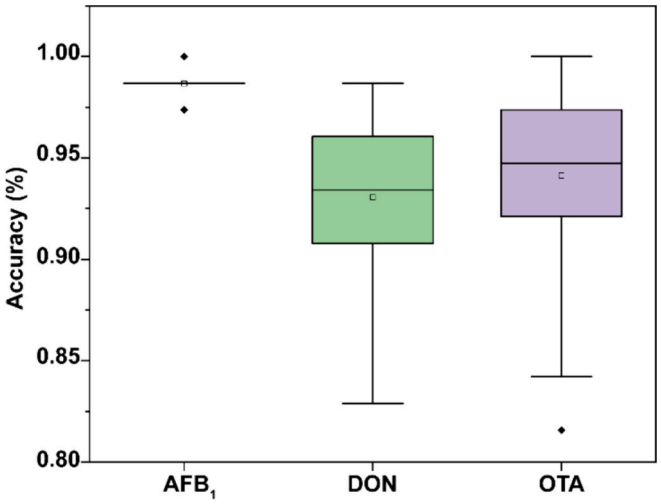

Fig. 4. The boxplots of prediction accuracy for AFB_1, DON and OTA samples.

find a factor correlated with the differences. Based on this dataset, MPLSDA can point out the following input spectra belonging to which mycotoxin. These results demonstrated the feasibility of classifying mycotoxins.

After the identification of mycotoxins from each other, combining the differences between the SERS spectra of Fe_3O_4@PDA@Au with/without mycotoxin in the presence of higher concentration of mycotoxin (Fig. S9c) and the Raman spectra of mycotoxins (Fig. S9b), the characteristic peaks at 1345 cm ^{1}, 1364 cm ^{1} could be assigned to CH_3 bending of AFB_1 and DON respectively (J. Li et al., 2019), while the characteristic band at 1002 cm ^{1} belonged to the ring breathing model of OTA, based on the previous researches and Fig. S7b (Rostami et al., 2020). Further, we also tested the reproducibility of the SERS spectra obtained by Fe_3O_4@PDA@Au with/without mycotoxins, each of them was tested by five repeated samples, the results show a good reproducibility in different repetitions (Fig. S10).

3.5. *Mycotoxins detection*

We investigated the quantitative detection of mycotoxins using a SERS-based sensor with Fe_3O_4@PDA nanoparticles. Under optimized conditions, 7 mg of these nanoparticles were added to 5 mL of AFB_1 solutions at concentrations ranging from 1 to 10 ng/mL, stirred for 25 min and then magnetically collected. After redispersion and in situ preparation of Au nanoparticles, the resulting MPNc was analyzed using a Raman spectrometer to record the SERS spectra which included AFB_1. The intensity of the Raman peaks increased with AFB_1 concentration, with a clear difference occurring at 10 ng/mL. The characteristic AFB_1 band at 1345 cm 1 correlated linearly with the mycotoxin concentration and reached a detection limit of 0.84 ng/mL. (Fig. 5a-b). Considering the affinity of PDA to OTA and DON, we extended the detection to these mycotoxins under similar conditions. The characteristic peaks for DON and OTA were identified and showed good linear relationships with their concentrations (Fig. 5c-f).

There was an interesting phenomenon here. Due to the peak overlap between mycotoxins and PDA, increasing mycotoxin concentrations resulted in stronger adsorption by Fe_3O_4@PDA, which also enhanced the SERS signal of PDA. Additionally, there were some fluctuations in the SERS spectra, mostly because of the polymer conformational changes after mycotoxins interaction. These phenomena were also observed in previous reports, which used polymers as affinity agents for mycotoxins analysis (V. M. Szlag et al., 2018; Victoria M. Szlag et al., 2019).

The limit of detection (LOD) was calculated, the details of the calculation and the equation are described in the supporting information. According to the definition of the signal-to-noise method addressed by the International Union of Pure and Applied Chemistry (IUPAC) ("IUPAC compendium of chemical terminology the gold book," 2006), the LOD of the nanosensor for AFB_1, DON, and OTA were 0.84, 0.72, and 0.63 ng/mL, respectively. Compared with the maximum residue limits of AFB_1, DON, and OTA in the published regulations of China, the US,

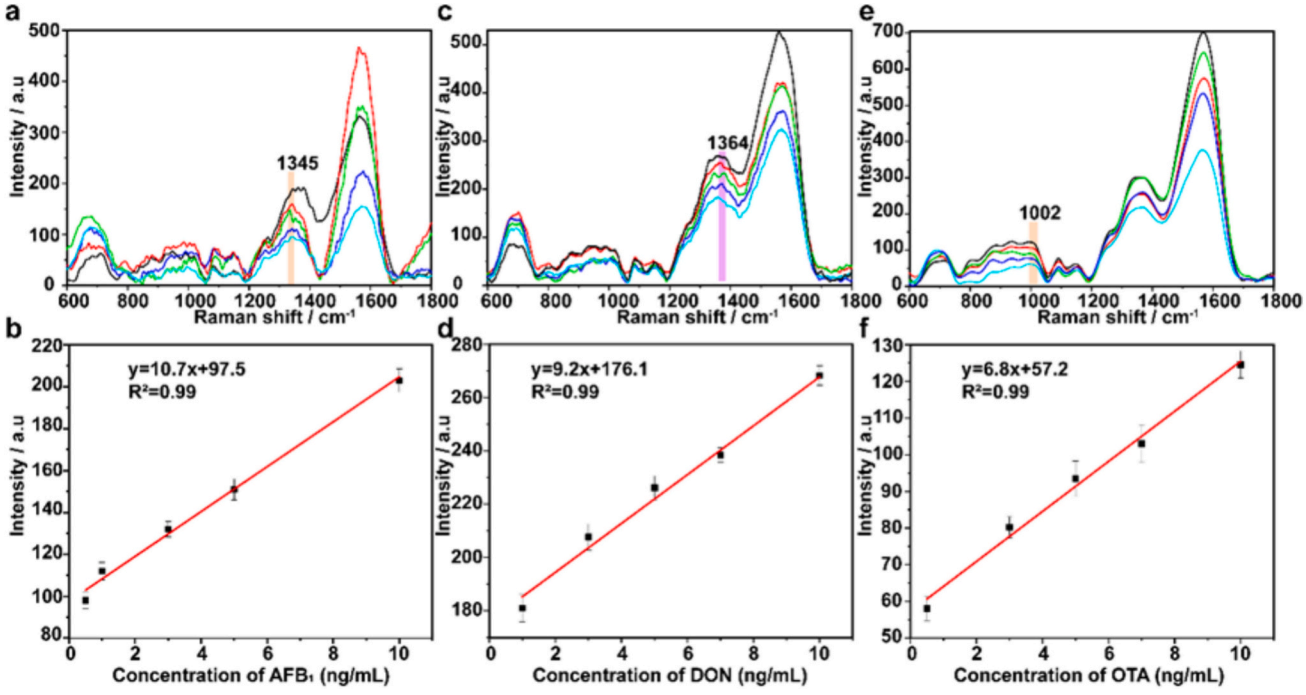

Fig. 5. (a) SERS spectra of AFB_1 with concentrations of 0.5, 1, 3, 5, and 10 ng/mL of standard work solutions. (c) SERS spectra of DON with concentrations of 1, 3, 5, 7, and 10 ng/mL of standard work solution. (e) SERS spectra of OTA with concentrations of 1, 3, 5, 7, and 10 ng/mL of standard work solution. Linear calibration curve between the SERS intensity and the concentrations of AFB_1 (b), DON (d), and OTA (f).

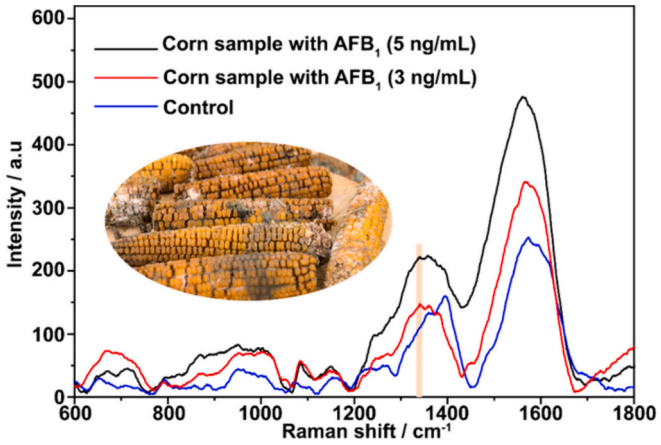

Fig. 6. SERS spectra of spiked corn samples with different concentrations of AFB_1 (5 ng/mL, 3 ng/mL) based on this nanosensor under optimal conditions for detection, compared with SERS spectra of Fe_3O_4@PDA nanoparticles as control.

and the European Union, the LOD values in this method are much less than these maximum residue limits (Table S4), reflecting the excellent performance of our nano-system in mycotoxin detection. We also compared the sensitivity with previous researches based on SERS fingerprinting detection (Table S6) and labeled SERS detection (Table S7), our method exhibited good sensitivity.

For further evaluation of the capability for real sample detection with multiple targets, spiked samples were used. We selected corn as a sample model spiked with different concentrations of AFB_1 (3 ng/mL, 5 ng/mL), and the spectra were obtained in Fig. 6. This was done by a blind test, the SERS spectra were identified by the MPLSDA analysis, the predication was same with the fact. Then we assigned the characteristic peak (1345 cm^{-1}) and calculated the amount of AFB_1 based on the standard curve. The recovery values obtained from the analysis were 92.4 ± 2.1%, and 93.6 ± 1.7%, respectively (Table S8). In the same way, the practical utility of our sensor for detecting OTA and DON was also evaluated, and the spectra were displayed in Fig. S11. The results listed in Table S8 show good recovery rate between 93.6 and 101.10%, with the relative deviation range of 2.1–4.8%, demonstrating the practicality and reliability of this sensor. In comparison to other methods, our nanosensor showed excellent sensing performance, suggesting the feasibility and potential applicability for the discrimination of multiple mycotoxins in real environmental samples.

4. Conclusions

This research provided a new SERS-based sensor for mycotoxins (AFB_1, OTA, DON) detection. Compared to previous sensors, our design described an overall more straightforward and efficient strategy that combined mycotoxin extraction, discrimination, and detection, which covered the whole process of mycotoxins analysis in corn samples. This was accomplished by a new design principle for the nanosensor operation: the nanosensor is formed directly and stepwise in the sample solutions to be analyzed without the need for lengthy and complicated sample pretreatments, with the LOD of ~1 ng/mL, satisfying the requirements of food authorities. Considering the significant and global problem of mycotoxin-related food poisoning, which requires rapid and often on-site detection of food samples, the nanosensor presented here offers the possibility of multiple robust and effective screening of food samples. Combing the adsorption of mycotoxin and formation of SERS substrate in situ, the entire procedure only needs 35 min, and the whole analysis will be finished in one hour. Although this research explored a new strategy for quantitatively detecting mycotoxins with a label-free SERS method assisted by MPLSDA, it is necessary to acknowledge that this study still have improvements. The ability of detecting mycotoxins simultaneously is still under investigated by developing a more powerful machine learning algorithm. The influence of mycotoxins on the formation of Au substrate and SERS stability are also need to be investigated.

Author contributions

The manuscript was written through contributions of all authors. All authors have given approval to the final version of the manuscript.

CRediT authorship contribution statement

Yang Zhang: Writing – original draft. **Chuping Zhao:** Investigation. **Pierre Picchetti:** Writing – review & editing. **Kaiyi Zheng:** Formal analysis. **Xinai Zhang:** Formal analysis. **Yanling Wu:** Data curation. **Ye Shen:** Formal analysis. **Luisa De Cola:** Investigation. **Jiyong Shi:** Resources. **Zhiming Guo:** Resources. **Xiaobo Zou:** Resources.

Declaration of competing interest

The authors declare that they have no known competing financial interests or personal relationships that could have appeared to influence the work reported in this paper.

Data availability

Data will be made available on request.

Acknowledgements

The authors gratefully acknowledge the financial support provided by Natural Science Foundation of Jiangsu Province (BK20210748) and Advanced Talents Science Foundation of Jiangsu University (No. 21JDG055).

References

Almeida, F., Rodrigues, M. L., & Coelho, C. (2019). The still underestimated problem of fungal diseases worldwide. *Frontiers in Microbiology, 10*, 214. https://doi.org/10.3389/fmicb.2019.00214

Andreasen, S. Z., Sanger, K., Jendresen, C. B., Nielsen, A. T., Emnéus, J., Boisen, A., & Zór, K. (2018). Extraction, enrichment, and in situ electrochemical detection on lab-on-a-disc: Monitoring the production of a bacterial secondary metabolite. *ACS Sensors, 4*, 398–405. https://doi.org/10.1021/acssensors.8b01277

Aragay, G., Pino, F., & Merkoçi, A. (2012). Nanomaterials for sensing and destroying pesticides. *Chemical Reviews, 112*, 5317–5338. https://doi.org/10.1021/cr300020c

Avery, S. V., Singleton, I., Magan, N., & Goldman, G. H. (2019). The fungal threat to global food security. *Fungal Biology, 123*, 555–557. https://doi.org/10.1016/j.funbio.2019.03.006

Bräse, S., Encinas, A., Keck, J., & Nising, C. F. (2009). Chemistry and biology of mycotoxins and related fungal metabolites. *Chemical Reviews, 109*, 3903–3990. https://doi.org/10.1021/cr050001f

Casadevall, A. (2018). Fungal diseases in the 21st century: The near and far horizons. *Pathogens and Immunity, 3*, 183–196. https://doi.org/10.20411/pai.v3i2.249

Che, D., Cheng, J., Ji, Z., Zhang, S., Li, G., Sun, Z., & You, J. (2017). Recent advances and applications of polydopamine-derived adsorbents for sample pretreatment. *TrAC Trends in Analytical Chemistry, 97*, 1–14. https://doi.org/10.1016/j.trac.2017.08.002

Choi, C. K. K., Chiu, Y. T. E., Zhuo, X., Liu, Y., Pak, C. Y., Liu, X., & Choi, C. H. J. (2019). Dopamine-Mediated Assembly of Citrate-Capped Plasmonic Nanoparticles into Stable Core–Shell Nanoworms for Intracellular Applications. *ACS Nano, 13*, 5864–5884. https://doi.org/10.1021/acsnano.9b01591

Cortés, M. T., Vargas, C., Blanco, D. A., Quinchanegua, I. D., Cortés, C., & Jaramillo, A. M. (2019). Bioinspired Polydopamine synthesis and its electrochemical characterization. *Journal of Chemical Education, 96*, 1250–1255. https://doi.org/10.1021/acs.jchemed.8b00432

Dai, H., Liang, S., Shan, D., Zhang, Q., Li, J., Xu, Q., & Wang, C. (2022). Efficient and simple simultaneous adsorption removal of multiple aflatoxins from various liquid

foods. *Food Chemistry, 380*, Article 132176. https://doi.org/10.1016/j.foodchem.2022.132176
Ding, Y., Sun, Y., Liu, C., Jiang, Q. Y., Chen, F., & Cao, Y. (2023). SERS-based biosensors combined with machine learning for medical application. *ChemistryOpen, 12*, Article e202200192. https://doi.org/10.1002/open.202200192
Eskola, M., Kos, G., Elliott, C. T., Hajslova, J., Mayar, S., & Krska, R. (2020). Worldwide contamination of food-crops with mycotoxins: Validity of the widely cited "FAO estimate" of 25. *Critical Reviews in Food Science and Nutrition, 60*, 2773–2789. https://doi.org/10.1080/10408398.2019.1658570
Feng, S., Huang, S., Lin, D., Chen, G., Xu, Y., Li, Y., & Zeng, H. (2015). Surface-enhanced Raman spectroscopy of saliva proteins for the noninvasive differentiation of benign and malignant breast tumors. *International Journal of Nanomedicine, 10*, 537–547. https://doi.org/10.2147/ijn.S71811
Ho, C.-S., Jean, N., Hogan, C. A., Blackmon, L., Jeffrey, S. S., Holodniy, M., & Dionne, J. (2019). Rapid identification of pathogenic bacteria using Raman spectroscopy and deep learning. *Nature Communications, 10*, 4927. https://doi.org/10.1038/s41467-019-12898-9
Huang, D., Fu, H., Huang, J., Luo, L., Lei, H., Shen, Y., & Xu, Z. (2021). Mimotope-based immunoassays for the rapid analysis of mycotoxin: A review. *Journal of Agricultural and Food Chemistry, 69*, 11743–11752. https://doi.org/10.1021/acs.jafc.1c04169
Huang, X., Zhan, S., Xu, H., Meng, X., Xiong, Y., & Chen, X. (2016). Ultrasensitive fluorescence immunoassay for detection of ochratoxin a using catalase-mediated fluorescence quenching of CdTe QDs. *Nanoscale, 8*, 9390–9397. https://doi.org/10.1039/C6NR01136E
Kasera, S., Biedermann, F., Baumberg, J. J., Scherman, O. A., & Mahajan, S. (2012). Quantitative SERS using the sequestration of small molecules inside precise plasmonic nanoconstructs. *Nano Letters, 12*, 5924–5928. https://doi.org/10.1021/nl303345z
Kasoju, A., Shahdeo, D., Khan, A. A., Shrikrishna, N. S., Mahari, S., Alanazi, A. M., & Gandhi, S. (2020). Fabrication of microfluidic device for aflatoxin M1 detection in milk samples with specific aptamers. *Scientific Reports, 10*, 4627. https://doi.org/10.1038/s41598-020-60926-2
Kasoju, A., Shrikrishna, N. S., Shahdeo, D., Khan, A. A., Alanazi, A. M., & Gandhi, S. (2020). Microfluidic paper device for rapid detection of aflatoxin B1 using an aptamer based colorimetric assay. *RSC Advances, 10*, 11843–11850. https://doi.org/10.1039/D0RA00062K
Kumar, A., Kumar, S., Rhim, W. K., Kim, G. H., & Nam, J. M. (2014). Oxidative nanopeeling chemistry-based synthesis and photodynamic and photothermal therapeutic applications of plasmonic core-petal nanostructures. *Journal of the American Chemical Society, 136*, 16317–16325. https://doi.org/10.1021/ja5085699
Kutsanedzie, F. Y. H., Agyekum, A. A., Annavaram, V., & Chen, Q. (2020). Signal-enhanced SERS-sensors of CAR-PLS and GA-PLS coupled AgNPs for ochratoxin a and aflatoxin B1 detection. *Food Chemistry, 315*, Article 126231. https://doi.org/10.1016/j.foodchem.2020.126231
Lee, K. M., Davis, J., Herrman, T. J., Murray, S. C., & Deng, Y. (2015). An empirical evaluation of three vibrational spectroscopic methods for detection of aflatoxins in maize. *Food Chemistry, 173*, 629–639. https://doi.org/10.1016/j.foodchem.2014.10.099
Lenzi, E., Henriksen-Lacey, M., Molina, B., Langer, J., de Albuquerque, C. D. L., Jimenez de Aberasturi, D., & Liz-Marzan, L. M. (2022). Combination of live cell surface-enhanced Raman scattering imaging with Chemometrics to study intracellular nanoparticle dynamics. *ACS Sensors, 7*, 1747–1756. https://doi.org/10.1021/acssensors.2c00610
Li, J., Wang, W., Zhang, H., Lu, Z., Wu, W., Shu, M., & Han, H. (2020). Programmable DNA tweezer-actuated SERS probe for the sensitive detection of AFB1. *Analytical Chemistry, 92*, 4900–4907. https://doi.org/10.1021/acs.analchem.9b04822
Li, J., Yan, H., Tan, X., Lu, Z., & Han, H. (2019). Cauliflower-inspired 3D SERS substrate for multiple mycotoxins detection. *Analytical Chemistry, 91*, 3885–3892. https://doi.org/10.1021/acs.analchem.8b04622
Li, Q., Wang, T., Hou, Y., Wang, D., Xiong, S., Wei, C., & Wang, F. (2023). Solid-phase extraction and simultaneous fluorescence detection of Cis-diol-containing biomolecules based on a novel Boronate affinity material. *Chromatographia, 86*, 387–399. https://doi.org/10.1007/s10337-023-04252-5
Liebscher, J., Mrówczyński, R., Scheidt, H. A., Filip, C., Hădade, N. D., Turcu, R., & Beck, S. (2013). Structure of Polydopamine: A never-ending story? *Langmuir, 29*, 10539–10548. https://doi.org/10.1021/la4020288
Liu, J., Sun, Z., Deng, Y., Zou, Y., Li, C., Guo, X., & Zhao, D. (2009). Highly water-dispersible biocompatible magnetite particles with low cytotoxicity stabilized by citrate groups. *Angewandte Chemie International Edition, 48*, 5875–5879. https://doi.org/10.1002/anie.200901566
Liu, X., Ying, G., Liao, X., Sun, C., Wei, F., Xing, X., & Zhou, L. (2019). Cytometric microbead magnetic suspension Array for high-throughput ultrasensitive detection of aflatoxin B1. *Analytical Chemistry, 91*, 1194–1202. https://doi.org/10.1021/acs.analchem.8b05278
Liu, Z., Wang, Y., Deng, R., Yang, L., Yu, S., Xu, S., & Xu, W. (2016). Fe3O4@graphene oxide@ag particles for surface magnet solid-phase extraction surface-enhanced Raman scattering (SMSPE-SERS): From sample pretreatment to detection all-in-one. *ACS Applied Materials & Interfaces, 8*, 14160–14168. https://doi.org/10.1021/acsami.6b02944
Ma, J.-X., Yang, H., Li, S., Ren, R., Li, J., Zhang, X., & Ma, J. (2015). Well-dispersed graphene-polydopamine-Pd hybrid with enhanced catalytic performance. *RSC Advances, 5*, 97520–97527. https://doi.org/10.1039/C5RA13361K
Mahoney, N., & Molyneux, R. J. (2010). Rapid analytical method for the determination of aflatoxins in plant-derived dietary supplement and cosmetic oils. *Journal of Agricultural and Food Chemistry, 58*, 4065–4070. https://doi.org/10.1021/jf9039028
McCullum, C., Tchounwou, P., Ding, L. S., Liao, X., & Liu, Y. M. (2014). Extraction of aflatoxins from liquid foodstuff samples with polydopamine-coated superparamagnetic nanoparticles for HPLC-MS/MS analysis. *Journal of Agricultural and Food Chemistry, 62*, 4261–4267. https://doi.org/10.1021/jf501659m
Molloy, S. F., Chiller, T., Greene, G. S., Burry, J., Govender, N. P., Kanyama, C., & Loyse, A. (2017). Cryptococcal meningitis: A neglected NTD? *PLoS Neglected Tropical Diseases, 11*, Article e0005575. https://doi.org/10.1371/journal.pntd.0005575
Munkvold, G. P., Arias, S., Taschl, I., & Gruber-Dorninger, C. (2019). Chapter 9 - mycotoxins in corn: Occurrence, impacts, and management. In S. O. Serna-Saldivar (Ed.), *Corn* (3rd ed., pp. 235–287). Oxford: AACC International Press.
Panikkanvalappil, S. R., Garlapati, C., Hooshmand, N., Aneja, R., & El-Sayed, M. A. (2019). Monitoring the dynamics of hemeoxygenase-1 activation in head and neck cancer cells in real-time using plasmonically enhanced Raman spectroscopy. *Chemical Science, 10*, 4876–4882. https://doi.org/10.1039/c9sc00093c
Phan-Quang, G. C., Wee, E. H. Z., Yang, F., Lee, H. K., Phang, I. Y., Feng, X., & Ling, X. Y. (2017). Online flowing Colloidosomes for sequential multi-analyte high-throughput SERS analysis. *Angewandte Chemie International Edition, 56*, 5565–5569. https://doi.org/10.1002/anie.201702374
Pomerantsev, A. L., & Rodionova, O. Y. (2018). Multiclass partial least squares discriminant analysis: Taking the right way—A critical tutorial. *Journal of Chemometrics, 32*. https://doi.org/10.1002/cem.3030
Rostami, S., Zór, K., Zhai, D. S., Viehrig, M., Morelli, L., Mehdinia, A., & Boisen, A. (2020). High-throughput label-free detection of Ochratoxin a in wine using supported liquid membrane extraction and ag-capped silicon nanopillar SERS substrates. *Food Control, 113*, Article 107183. https://doi.org/10.1016/j.foodcont.2020.107183
dos Santos, D. P., Sena, M. M., Almeida, M. R., Mazali, I. O., Olivieri, A. C., & Villa, J. E. L. (2023). Unraveling surface-enhanced Raman spectroscopy results through chemometrics and machine learning: Principles, progress, and trends. *Analytical and Bioanalytical Chemistry, 415*, 3945–3966. https://doi.org/10.1007/s00216-023-04620-y
Sun, C., Yuan, F., Li, H., & Wu, X. (2018). A specific fluorescent nanoprobe for dopamine based on the synergistic action of citrate and gold nanoparticles on Tb(III) luminescence. *Microchimica Acta, 185*, 317. https://doi.org/10.1007/s00604-018-2844-0
Szlag, V. M., Jung, S., Rodriguez, R. S., Bourgeois, M., Bryson, S., Schatz, G. C., & Haynes, C. L. (2018). Isothermal titration calorimetry for the screening of aflatoxin B1 surface-enhanced Raman scattering sensor affinity agents. *Analytical Chemistry, 90*, 13409–13418. https://doi.org/10.1021/acs.analchem.8b03221
Szlag, V. M., Rodriguez, R. S., Jung, S., Bourgeois, M. R., Bryson, S., Purchel, A., & Reineke, T. M. (2019). Optimizing linear polymer affinity agent properties for surface-enhanced Raman scattering detection of aflatoxin B1. *Molecular Systems Design & Engineering, 4*, 1019–1031. https://doi.org/10.1039/c9me00032a
Wan, H., Zhang, B., Bai, X. L., Zhao, Y., Xiao, M. W., & Liao, X. (2017). Extraction of ochratoxin a in red wine with dopamine-coated magnetic multi-walled carbon nanotubes. *Journal of Separation Science, 40*, 4022–4031. https://doi.org/10.1002/jssc.201700697
Wang, F., Xiong, S., Wang, T., Hou, Y., & Li, Q. (2023). Discrimination of cis-diol-containing molecules using fluorescent boronate affinity probes by principal component analysis. *Analytical Methods, 15*, 5803–5812. https://doi.org/10.1039/D3AY01719B
Wang, L., Zhu, F., Chen, M., Xiong, Y., Zhu, Y., Xie, S., & Chen, X. (2019). Development of a "dual gates" locked, target-triggered Nanodevice for point-of-care testing with a glucometer readout. *ACS Sensors, 4*, 968–976. https://doi.org/10.1021/acssensors.9b00072
Wang, Y., Xu, J., Cui, D., Kong, L., Chen, S., Xie, W., & Zhang, C. (2021). Classification and identification of Archaea using single-cell Raman ejection and artificial intelligence: Implications for investigating uncultivated microorganisms. *Analytical Chemistry, 93*, 17012–17019. https://doi.org/10.1021/acs.analchem.1c03495
Wu, Z., Pu, H., & Sun, D.-W. (2021). Fingerprinting and tagging detection of mycotoxins in Agri-food products by surface-enhanced Raman spectroscopy: Principles and recent applications. *Trends in Food Science & Technology, 110*, 393–404. https://doi.org/10.1016/j.tifs.2021.02.013
Xiong, Y., Li, W., Wen, Q., Xu, D., Ren, J., & Lin, Q. (2022). Aptamer-engineered nanomaterials to aid in mycotoxin determination. *Food Control, 135*, Article 108661. https://doi.org/10.1016/j.foodcont.2021.108661
Yang, L., Wei, F., Liu, J.-M., & Wang, S. (2021). Functional hybrid Micro/Nanoentities promote agro-food safety inspection. *Journal of Agricultural and Food Chemistry, 69*, 12402–12417. https://doi.org/10.1021/acs.jafc.1c05185
Yang, Y., Su, Z., Wu, D., Liu, J., Zhang, X., Wu, Y., & Li, G. (2022). Low background interference SERS aptasensor for highly sensitive multiplex mycotoxin detection based on polystyrene microspheres-mediated controlled release of Raman reporters. *Analytica Chimica Acta, 1218*, Article 340000. https://doi.org/10.1016/j.aca.2022.340000
Ye, Q., Zhou, F., & Liu, W. (2011). Bioinspired catecholic chemistry for surface modification. *Chemical Society Reviews, 40*, 4244–4258. https://doi.org/10.1039/C1CS15026J
Yin, L., You, T., El-Seedi, H. R., El-Garawani, I. M., Guo, Z., Zou, X., & Cai, J. (2022). Rapid and sensitive detection of zearalenone in corn using SERS-based lateral flow immunosensor. *Food Chemistry, 396*, Article 133707. https://doi.org/10.1016/j.foodchem.2022.133707
Yu, S., Li, G., Liu, R., Ma, D., & Xue, W. (2018). Dendritic Fe_3O_4@poly(dopamine)@PAMAM nanocomposite as controllable NO-releasing material: A synergistic Photothermal and NO antibacterial study. *Advanced Functional Materials, 28*, 1707440. https://doi.org/10.1002/adfm.201707440

Zhang, W., Tang, S., Jin, Y., Yang, C., He, L., Wang, J., & Chen, Y. (2020). Multiplex SERS-based lateral flow immunosensor for the detection of major mycotoxins in maize utilizing dual Raman labels and triple test lines. *Journal of Hazardous Materials, 393*, Article 122348. https://doi.org/10.1016/j.jhazmat.2020.122348

Zhang, Y., Wang, Z., Wu, L., Zong, S., Yun, B., & Cui, Y. (2018). Combining multiplex SERS Nanovectors and multivariate analysis for in situ profiling of circulating tumor cell phenotype using a microfluidic Chip. *Small, 14*, Article e1704433. https://doi.org/10.1002/smll.201704433

Zhao, Y., Yang, Y., Luo, Y., Yang, X., Li, M., & Song, Q. (2015). Double detection of mycotoxins based on SERS labels embedded ag@au Core-Shell nanoparticles. *ACS Applied Materials & Interfaces, 7*, 21780–21786. https://doi.org/10.1021/acsami.5b07804

Zheng, R., Wang, S., Tian, Y., Jiang, X., Fu, D., Shen, S., & Yang, W. (2015). Polydopamine-coated magnetic composite particles with an enhanced Photothermal effect. *ACS Applied Materials & Interfaces, 7*, 15876–15884. https://doi.org/10.1021/acsami.5b03201

Zhou, S., Guo, X., Huang, H., Huang, X., Zhou, X., Zhang, Z., & Sun, P. (2022). Triple-function au-ag-stuffed Nanopancakes for SERS detection, discrimination, and inactivation of multiple Bacteria. *Analytical Chemistry, 94*, 5785–5796. https://doi.org/10.1021/acs.analchem.1c04920

Zhou, S., Xu, L., Kuang, H., Xiao, J., & Xu, C. (2020). Immunoassays for rapid mycotoxin detection: State of the art. *Analyst, 145*, 7088–7102. https://doi.org/10.1039/D0AN01408G